Journal of Organometallic Chemistry 694 (2009) 3506–3510

Contents lists available at ScienceDirect

Journal of Organometallic Chemistry

journal homepage: www.elsevier.com/locate/jorganchem

Group 9 half-sandwich complexes containing the unique *P,P′*-diphenyl-1,4-diphospha-cyclohexane ligand: Synthesis, X-ray structure analyses and spectroscopic studies

Joshua E. Sussman [a], Tara S. Morey [a], Susie M. Miller [b], Monte L. Helm [a,*]

[a] Chemistry Department, Fort Lewis College, 1000 Rim Drive, Durango, CO 81301, USA
[b] Department of Chemistry, Colorado State University, Fort Collins, CO 80523, USA

ARTICLE INFO

Article history:
Received 17 March 2009
Received in revised form 17 June 2009
Accepted 19 June 2009
Available online 24 June 2009

Keywords:
P,P′-diphenyl-1,4-diphospha-cyclohexane
Rhodium complexes
Iridium complexes
Mixed sandwich complexes
Phosphine ligands
Pentamethylcyclopentadienide complexes

ABSTRACT

We wish to report the synthesis and characterization of Group 9 metal complexes with the novel *P,P′*-diphenyl-1,4-diphospha-cyclohexane (dpdpc) ligand. The complexes are readily prepared by direct ligand substitution reactions from the dichloro-bridged binuclear complexes, $[\{\eta^5\text{-Cp}^*\text{M(Cl)}_2\}_2]$. The complexes include: $[\eta^5\text{-Cp}^*\text{Rh(Cl)}_2]_2(\mu\text{-dpdpc})$ (**1**), $[\eta^5\text{-Cp}^*\text{Ir(Cl)}_2]_2(\mu\text{-dpdpc})$ (**2**), and $[\eta^5\text{-Cp}^*\text{Rh(Cl)(dpdpc)}]\text{PF}_6$ (**3**). The structures for all three complexes are supported by ^{1}H, ^{13}C{^{1}H}, and ^{31}P{^{1}H} NMR spectroscopy as well as elemental analysis. The molecular structures of **1** and **3** have also been established by single-crystal X-ray analysis.

1. Introduction

Over the years, phosphine ligands have played an essential role in the development of metal-mediated catalysis [1–6]. The ability to form a wide variety of sterically and electronically unique phosphine ligands has lead to a pleathora of information about how to influence catalytic cycles. For example, the role of the P–M–P bite angle in migratory insertion of ethylene and carbon monoxide in palladium complexes has been well documented [7]. Additionally, a recent review documents the influence of phosphine ligand bite angle in a variety of metal catalyzed carbon–carbon bond formation reactions [8]. The ability to synthesize phosphine ligands with unique electronic and steric properties continues to be an important piece in catalytic development.

Although there exists a large body of knowledge in the literature on bidentate phosphine ligands with a single bridging carbon chain (i.e. $R_2P\text{–C–C–}PR_2$), very little research has been done on cyclic bidentate phosphines with two connecting carbon chains (i.e. $RP(\text{–C–C–})_2PR$). Such compounds are of particular interest due to the fact that the phosphorus atoms are held in a rigid steric position that could lead to distorted metal coordination geometries and different reaction chemistry than seen in their acyclic counterparts. One cyclic bidentate phosphine ligand that shows potential for interesting metal coordination behavior is *P,P′*-diphenyl-1,4-diphospha-cyclohexane (dpdpc) [9]. Synthesis of the dpdpc ligand results in formation of both *cis*- and *trans*-isomers as shown in Fig. 1. Previous work conducted by Panunzi et al. on the metal coordination properties of this ligand demonstrate its versatility towards binding M(II) centers (M = Co, Ni, Pd and Pt) [10]. Furthermore, previous work from our laboratories have resulted in the formation and structural characterization of $[M(dpdpc)_2]Cl_2$, (M = Pd, Pt) complexes [11,12]. Interestingly, these complexes show an average 73° P–M–P bite angle, much smaller then that for typical acyclic bidentate phosphines.

The interesting coordination properties of the dpdpc ligand have lead us to focus our attention on further understanding the steric and electronic coordination properties of this compound. A study completed by De Fraldi and Roviello indicated Group 10 metal coordination of the dpdpc ligand can be influenced by the charge of the metal center [13]. Their research indicated cationic Group 10 metal centers preferred chelation by the dpdpc ligand, where neutral metal centers preferred binucleation through a bridging dpdpc ligand. The unique and varying coordination modes of the dpdpc ligand has lead us to focus our attention on extending the metal coordination of the dpdpc ligand to Group 9 metal centers [14,15].

In this work we have synthesized three new coordination compounds of the dpdpc ligand with Rh(III) and Ir(III) metal centers

* Corresponding author. Tel.: +1 970 247 7635; fax: +1 970 247 7567.
E-mail address: helm_m@fortlewis.edu (M.L. Helm).

0022-328X/$ - see front matter © 2009 Elsevier B.V. All rights reserved.
doi:10.1016/j.jorganchem.2009.06.023

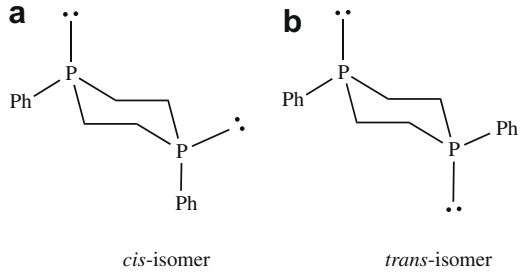

Fig. 1. Structure of the (a) *cis*-dpdpc and (b) *trans*-dpdpc ligand.

and the η^5-pentamethylcyclopentadienide (Cp*) ligand. The data reported herein indicate the Rh(III) monomeric cationic complex of dpdpc is formed through a bridged dimeric intermediate. X-ray crystal structures of the dimeric $[Cp^*Rh(Cl)_2]_2$(μ-dpdpc) and monomeric [Cp*Rh(Cl)(dpdpc)][PF_6] will be reported.

2. Experimental

2.1. General remarks

Standard procedures for the manipulation of air-sensitive materials were employed. Unless stated otherwise, all manipulations were carried out at ambient temperature under an atmosphere of dry argon or nitrogen gas using standard Schlenk, syringe and high-vacuum line techniques. All solvents were dried and distilled prior to use. The ruthenium, $[Cp^*RhCl_2]_2$, and iridium, $[Cp^*IrCl_2]_2$, starting compounds (*Sigma–Aldrich*) were purchased and used as received. Elemental analyses of the complexes were performed by Huffman Laboratories in Goldon, CO USA. The NMR spectra were recorded on a JEOL ESX-400 MHz instrument and referenced using external standards. Infrared spectra were recorded on a Thermo Nicolet Avatar 360 FT-IR spectrophotometer. The dpdpc ligand was made according to literature procedure [9].

2.2. Preparation of complexes **1–3**

2.2.1. Synthesis of $[Cp^*Rh(Cl)_2]_2$(μ-dpdpc) (**1**)

A mixture of $[Cp^*RhCl_2]_2$ (0.151 g, 0.25 mmol) and dpdpc ligand (0.068 g, 0.25 mmol) in 25 mL of degassed ethanol was refluxed under N_2 for 2 h, after which an orange precipitate formed. The dark orange solid was filtered and dried under vacuum, leaving 100 mg (45% yield). Anal. Calc. for $C_{36}H_{48}Cl_4P_2Rh_2$: C, 48.56; H, 5.43. Found: C, 48.20; H, 5.68%. *cis*-Isomer (**1a**) ^{1}H NMR ($CDCl_3$): δ, 7.67–7.29 (m, C_6H_5, 10H); 3.69 and 2.37 (m, –CH_2–, 8H); 1.38 (m, –CH_3, 30H). $^{13}C\{^1H\}$ NMR ($CDCl_3$): δ, 132.7, 131.1, 130.4 and 128.5 (m, C_6H_5, 12C); 98.6 (m, *C*p*, 5C); 19.3 (m, *C*H_2, 4C); 9.01 (s, –CH_3, 10C). $^{31}P\{^1H\}$ NMR ($CDCl_3$): δ, 14.1 (d, $^1J_{Rh-P}$ = 138.7 Hz, 2P). *trans*-isomer (**1b**) $^{31}P\{^1H\}$ NMR ($CDCl_3$): δ, 18.0 (d, $^1J_{Rh-P}$ = 138.7 Hz, 2P).

2.2.2. Synthesis of $[Cp^*Ir(Cl)_2]_2$(μ-dpdpc) (**2**)

A solution of dpdpc (0.038 g, 0.125 mmol) in 3.75 mL CH_2Cl_2 was added dropwise to a solution of $[Cp^*IrCl_2]_2$ (0.100 g, 0.125 mmol) in 3.15 mL CH_2Cl_2 that was cooled to 0 °C. The mixture was then stirred overnight. The next morning the volume was reduced by half, approximately 3 mL of ethanol was added, followed by removal of solvents until an orange precipitate formed. The orange solid was filtered, washed with ethanol and dried with ether giving 69 mg of product (52% yield). Anal. Calc. for $C_{36}H_{48}Cl_4P_2Rh$: C, 40.45; H, 4.53. Found: C, 40.11; H, 4.55%. *cis*-Isomer (**2a**) ^{1}H NMR ($CDCl_3$): δ, 7.33–7.56 (m, C_6H_5, 10H); 3.55 and 2.55 (m, –CH_2–, 8H); 1.32 (m, –CH_3, 30H). $^{13}C\{^1H\}$ NMR ($CDCl_3$): δ, 133.1, 131.5, 130.8, 128.8 (m, C_6H_5, 12C); 92.2 (s, *C*p*, 10C); 19.3 (m, –CH_2–, 4C); 8.67 (s, –CH_3, 10C). $^{31}P\{^1H\}$ NMR ($CDCl_3$): δ, −19.6 (s, 2P). *trans*-isomer (**2b**) $^{31}P\{^1H\}$ NMR ($CDCl_3$): δ, −15.3 (s, 2P).

2.2.3. Synthesis of [Cp*Rh(Cl)(dpdpc)][PF_6] (**3**)

A mixture of $[Cp^*RhCl_2]_2$ (0.151 g, 0.25 mmol) and dpdpc (0.322 g, 1.18 mmol) in 50 mL of degassed ethanol was refluxed under N_2 for 3 h after which the solution had turned bright red/orange. Solvent was removed via vacuum and 8.5 mL of degassed ethanol followed by a solution of ammonium hexafluorophosphate (170 mg in 8.5 mL water) was added. A red precipitate formed, was filtered and dried under vacuum leaving 48 mg (28% yield). Anal. Calc. for $C_{26}H_{33}ClF_6P_3Rh$: C, 45.20; H, 4.81. Found: C, 45.28; H, 4.93%. ^{1}H NMR ($CDCl_3$): δ, 7.75–7.58 (C_6H_5, m, 10H); 2.96, 2.58 and 2.32 (CH_2, m, 8H); 1.44 (Cp*–CH_3, s, 15H). $^{13}C\{^1H\}$ NMR ($CDCl_3$): δ, 133.2, 131.3, 129.8, and 124.2 (m, C_6H_5, 6C); 103.2 (m, Cp*, 5C); 25.2 and 21.3 (m, –CH_2–, 4C); 9.01 (s, –CH_3, 5C). $^{31}P\{^1H\}$ NMR ($CDCl_3$): δ, 67.0 (d, $^1J_{Rh-P}$ = 125.7 Hz, 2P); −143.7 (sept., PF_6, $^1J_{P-F}$ = 715.3 Hz, 1P).

2.3. Single crystal X-ray structure analyses

X-ray quality crystals of the complexes **1b** and **3** were grown by slow evaporation of THF from a solution of the compounds. X-ray intensity data were collected on a standard SMART 1K CCD diffractometer using graphite-monochromated Mo Kα radiation, λ = 0.71073 Å. Absorption and other corrections were applied using SADABS [16]. In all cases the space group was determined by observation of systematic absences and intensity statistics. Structures were solved by direct methods using SHELXTL and refined by full-matrix least squares on F^2 [17]. Crystallographic details are summarized in Table 1.

Table 1
Crystallographic and structure refinement parameters for **1** and **3**.

	$[Cp^*Rh(Cl)_2]_2$ (dpdpc) (**1**)	[Cp*Rh(Cl)(dpdpc)][PF_6] (**3**)
Chemical formula	$C_{18}H_{24}Cl_2PRh$	$C_{30}H_{41}ClF_6OP_3Rh$
Formula weight	445.15	762.90
Crystal system	Triclinic	Monoclinic
Space Group	$P\bar{1}$	$P2(1)$
Crystal color and shape	Orange hexagonal plate	Orange rod
Crystal size (mm^3)	0.20 × 0.12 × 0.05	0.60 × 0.08 × 0.07
a (Å)	8.7058(6)	10.2073(5)
b (Å)	13.6352(10)	8.5765(5)
c (Å)	16.4117(12)	18.8761(10)
α (°)	71.103(4)	90
β (°)	86.161(4)	99.420(3)
γ (°)	85.464(4)	90
V (Å^3)	1835.6(2)	1630.19(15)
Z	4	2
D_{calc} (Mg/m^3)	1.611	1.554
μ (mm^{-1})	1.303	0.811
Scan range (°)	1.58 < θ < 33.35	2.02 < θ < 33.36
Reflections collected	67 364	20 635
Independent reflections	14 122	11 031
R_{int}	0.0408	0.0357
Final *R* indices [$I > 2\sigma(I)$][a]	R_1 = 0.0315, wR_2 = 0.0789	R_1 = 0.0396, wR_2 = 0.0892
R indices (all data)[a]	R_1 = 0.0446, wR_2 = 0.0885	R_1 = 0.0497, wR_2 = 0.0943
Goodness-of-fit (GOF) on F^2	0.824	0.965
Maximum, minimum Δρ (e Å^{-3})	1.209, −1.150	1.271, −0.641

[a] $R_1 = \sum ||F_o| - |F_c|| / \sum |F_o|$. $wR_2 = \left[\sum w(|F_o| - |F_c|)^2 / \sum w(F_o)^2\right]^{1/2}$.

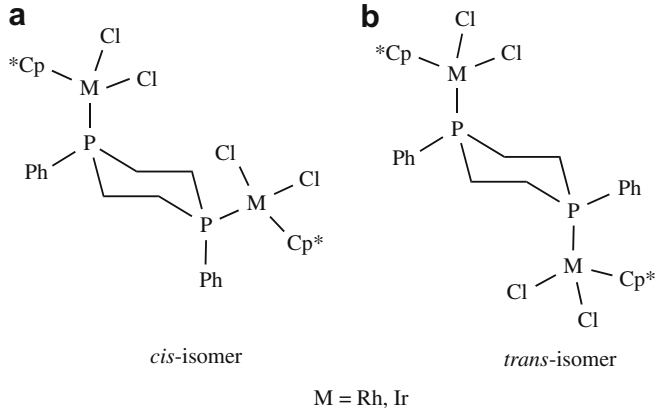

Fig. 2. Structure of the (a) *cis*- and (b) *trans*-isomers of **1** and **2**.

3. Results and discussion

3.1. Syntheses and NMR spectroscopy

The reaction of the dimeric chloro-bridged metal complexes, $[Cp^*M(\mu\text{-}Cl)Cl]_2$ (M = Rh, Ir), with a stoichiometric amount of the dpdpc ligand results in formation of the dimeric diphosphine-bridged complexes of general type $[Cp^*M(Cl)_2]_2(\mu\text{-dpdpc})$ (**1**, **2**) as shown in Eq. (1).

$$[Cp^*M(\mu\text{-}Cl)Cl]_2 + \text{dpdpc} \rightarrow [Cp^*M(Cl)_2]_2(\mu\text{-dpdpc}) \quad M = \text{Rh}(\mathbf{1}); \mathbf{Ir}(\mathbf{2}) \tag{1}$$

The synthesis of compounds **1** and **2** result in formation of two distinct isomers arising from the configuration of the 6-membered ring of the phosphorus ligand, the major (*cis*) isomer and minor (*trans*) isomer (**a** and **b**, respectively, Fig. 2). The configuration of the 6-membered ring of the phosphorus ligand can be inferred from the ratio of products, as the starting dpdpc ligand occurs in approximately the same 9:1 *cis*/*trans* ratio in the P-31 NMR. Further, through serendipitous crystallization, the minor *trans*-isomer of the Rh dimer (**1b**) was crystallized, which allowed for absolute assignment of their P-31 NMR peaks. The compounds are readily identified through their distinct $^{31}P\{^1H\}$ NMR spectra, that consist of a major peak for the *trans*-isomer and minor peak for the *cis*-isomer in approximately 9:1 ratio, as determined by P-31 NMR integration. Although P-31 NMR of the reactions mixtures shows quantitative formation of the products, the compounds are isolated in 40–50% yields as pure orange solids as characterized by their elemental analysis.' The isolated products are non-hydroscopic, air-stable solids, soluble in THF, acetonitrile and chlorinated solvents.

Compounds **1a** and **2a** are fully characterized through ^1H, ^{13}C and ^{31}P NMR, and elemental analysis. Attempts to isolate the *trans*-isomers (**1b**, **2b**) were unsuccessful, so their characterization relies only on P-31 NMR and elemental analysis of the bulk sample. The P-31 NMR spectra of all compounds show the expected downfield chemical shift from the free dpdpc ligand upon metal coordination (44 ppm average). Further evidence of metal coordination in compounds **1a** and **1b** is illustrated through the observation of J^1_{Rh-P} coupling of 137.8 Hz. Interestingly, there is no difference in the Rh–P coupling between the *cis*- and *trans*-isomers. The proton and carbon-13 NMR spectra of **1a** and **2a** show the correct number of peaks, splittings and intensities associated with the Cp*-ring and carbon backbone of the dpdpc ligand. The proton NMR of the dpdpc $-CH_2-$ carbon backbone appears as a pair of two distinct multiplets of approximate AA′BB′ splitting pattern. The magnetic inequivalency of these methylene protons are attributed to them being in fixed axial or equatorial positions (on the NMR time scale). There are no noteworthy differences between the proton and carbon-13 NMR spectra between the Rh(III) and Ir(III) complexes.

The reaction of the dimeric chloro-bridged metal complex $[Cp^*Rh(\mu\text{-}Cl)Cl]_2$ with an excess of the dpdpc ligand, and subsequent reaction with NH_4PF_6, results in formation of the monomeric diphosphine complex $[Cp^*Rh(Cl)(dpdpc)][PF_6]$ (**3**), as shown in Eq. (2). The formation of **3** in the reaction mixture can be monitored through appearance of a distinct singlet with Rh-coupled satellites in the P-31 NMR. The isolated orange solid is non-hydroscopic, air-stable, and soluble in THF, acetonitrile and chlorinated solvents.

$$[Cp^*Rh(\mu\text{-}Cl)Cl]_2 + \text{dpdpc (excess)} + NH_4PF_6 \rightarrow [Cp^*Rh(dpdpc)(Cl)][PF_6](\mathbf{3}) + \mathbf{NH_4Cl} \tag{2}$$

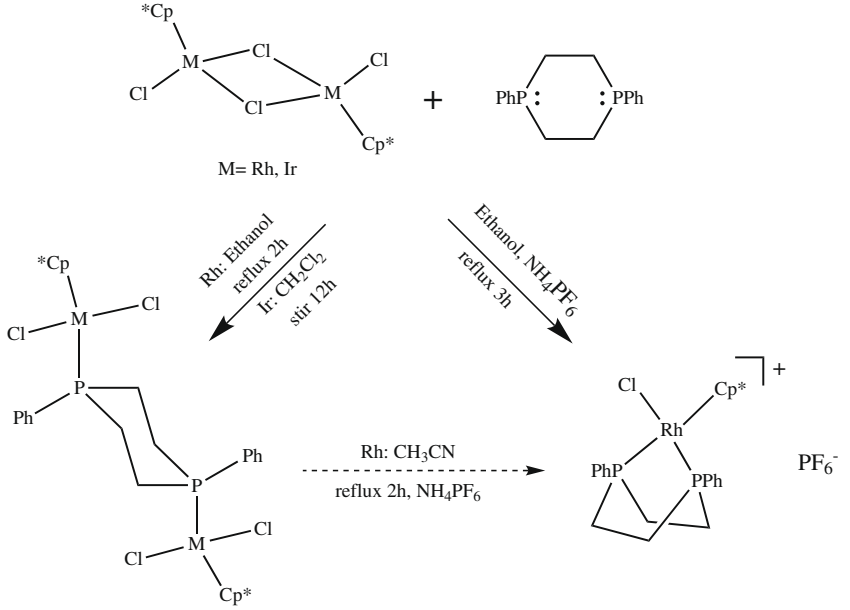

Scheme 1. Overall reaction summary.

Compound **3** is fully characterized through ^{1}H, ^{13}C and ^{31}P NMR, elemental analysis and X-ray crystallography. The P-31 NMR of **3** shows an expected downfield chemical shift from the free dpdpc ligand of 94 ppm and $^{1}J_{Rh-P}$ coupling of 125.7 Hz. The downfield chemical shift in **3** is approximately 50 ppm greater then the downfield chemical shift observed in **1** and **2**. The increase in the downfield chemical shift may be due to the phosphorus ligand's ability to function as a stronger sigma-donor to the rhodium with the loss of one additional chlorine, or the formation of a 5-membered chelate ring to one metal center. The P-31 NMR also shows the expected peaks for the ^{19}F coupled PF_6^- anion in the correct ratio. The proton and carbon-13 NMR spectra of **3** show the correct number of peaks, splittings and intensities associated with the Cp*-ring and carbon backbone of the dpdpc ligand. As observed in the dimeric-bridged compounds, proton NMR of the dpdpc $-CH_2-$ carbon backbone appears as a pair of two distinct multiplets of approximate AA'BB' splitting pattern.

In an attempt to understand the reaction progress for formation of the monomeric Rh-dpdpc complex (**3**), direct conversion of the dimeric-Rh complex **1** to monomeric **3** was explored. Refluxing **1** in acetonitrile results in the disappearance of the P-31 NMR peaks at 14.1 and 18.0 ppm (due to **1a/b**) and appearance of a peak at 67.0 ppm due to **3**. After 2 h of reflux time, conversion of **1**–**3** appears complete as analyzed by P-31 NMR. This data indicates that di-metallic bridged complex **1** can function as an intermediate in formation of **3**, as shown in Scheme 1. Conversion of **1** from **3** requires the loss of one metal center and, as a result, formation of a secondary metallic product is expected. Because this product does not contain phosphorus, its appearance is not observed in the P-31 NMR and no attempts were made to isolate it. Interestingly, we were unable to convert the di-metallic iridium complex (**2**) to the analogous monometallic complex, even with extended reflux times.

3.2. X-ray structural data

The structures of *trans*-[Cp*Rh(Cl)$_2$]$_2$(μ-dpdpc) (**1b**) and [Cp*Rh(Cl)(dpdpc)][PF_6] (**3**) were determined by single-crystal X-ray diffraction, as illustrated in Figs. 3 and 4, respectively. A crystallographic summary is given in Table 1, selected bond lengths and angles in Table 2. Both structures show facial coordination of the η^5-Cp* ligand in addition to 3-anciliary ligands, resulting in a six-coordinate distorted octahedral geometry around the Rh(III) center.

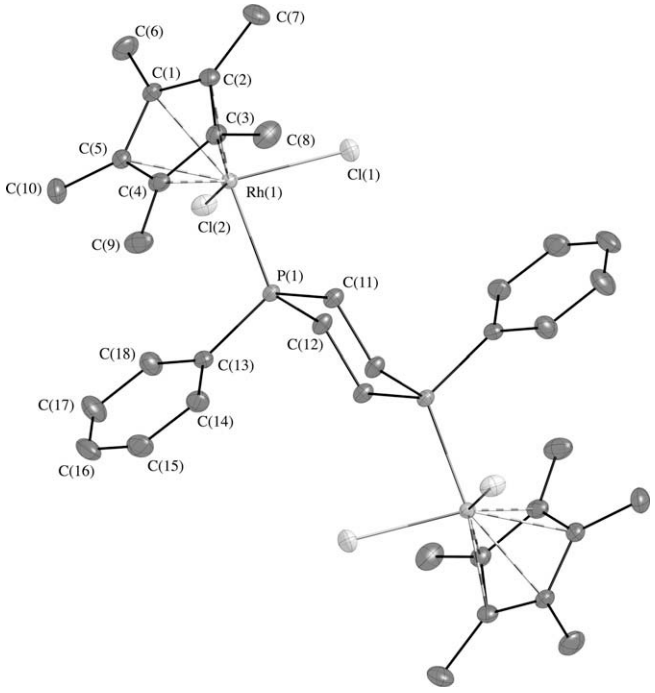

Fig. 3. Thermal ellipsoid perspective (50% probability) of **1b**.

Compound **1b** clearly shows the dpdpc ligand functioning in a bridging fashion between two Rh(III) metal centers. The bond angles between the Rh(III) metal center, the two chlorine ligands and phosphorus atom in the dpdpc ligand are all near the expected 90° values. The structure also shows the six-membered ring of the dpdpc ligand in the chair-type confirmation with coordination to

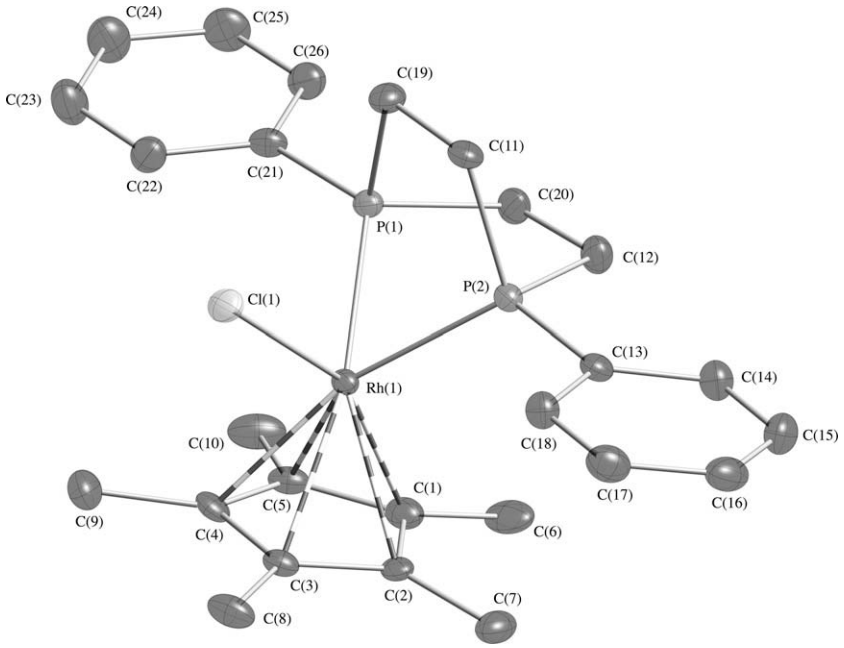

Fig. 4. Thermal ellipsoid perspective (50% probability) of cation of **3** (PF_6^- anion omitted for clarity).

Table 2
Selected bond distances (Å) and angles (°) for *trans*-[η_5-Cp*Rh(Cl)$_2$]$_2$(μ-dpdpc) (**1b**) and [η^5-Cp*Rh(Cl)(dpdpc)][PF_6] (**3**).

Distances (Å)	**1b**	**3**	Angles (°)	**1b**	**3**
Rh1–Cl1	2.4033(6)	2.4026(8)	*Around Rh1*		
Rh1–Cl2	2.4200(6)	–	Cl1–Rh1–Cl2	92.21(2)	–
Rh1–P1	2.2940(5)	2.2818(6)	Cl2–Rh1–P1	85.49(2)	–
Rh1–P2	–	2.2802(8)	Cl1–Rh1–P1	90.43(2)	92.14(3)
			P2–Rh1–Cl1	–	92.69(3)
P1–C11	1.826(2)	1.831(3)	P1–Rh1–P2	–	71.60(3)
P1–C12	1.823(2)	1.837(3)			
P1–C13	1.819(2)	1.794(3)	*Around P1*		
			Rh1–P1–C11	111.49(7)	106.80(10)
Cp–M distances			Rh1–P1–C12	112.83(7)	105.68(10)
Rh1–C1	2.141(2)	2.241(3)	Rh1–P1–C13	114.62(7)	122.83(9)
Rh1–C2	2.168(2)	2.226(3)	C11–P1–C12	103.51(9)	99.89(16)
Rh1–C3	2.162(2)	2.225(3)	C11–P1–C13	108.55(10)	108.86(15)
Rh1–C4	2.236(2)	2.169(3)	C12–P1–C13	105.06(10)	110.33(15)
Rh1–C5	2.231(2)	2.244(3)			

two metal centers in a *trans*-position. Until now the only structural reports containing the dpdpc ligand have been with the ligand in the boat-type confirmation bound to a metal in a bidentate fashion.

Compound **3** shows the dpdpc ligand bound in a bidentate fashion to the Rh metal center. The bond angles around the metal center in **3** are more distorted then observed in **1b**, with the most clear example being the acute 71.60° P–Rh–P bite angle. This acute bite angle observed when the dpdpc ligand binds in a bidentate way to a metal center has been reported in other dpdpc metal complexes. To the author's knowledge, complex **3** displays the smallest P–M–P bite angle of any 2-carbon bridged diphosphine (i.e. P–C–C–P) ligand to date. In addition to the acute bite angle, compound **3** displays shorter Rh–P bond distances that observed in **1b**. This is in agreement with the P-31 NMR data that shows the phosphorus atoms in **3** function as stronger sigma-donors to the Rh(III) center then observed in **1b**. These crystals structures support the idea that the dpdpc ligand is capable of functioning both as a strongly bound, bidentate chelating ligand as well as a bridging diphosphine ligand.

4. Conclusion

Herein, we reported the synthesis of a new series of RP(–C–C–)$_2$PR diphosphine complexes with rhodium(III) and iridium(III) metal centers. In this work we demonstrated the versatile coordination properties of the dpdpc ligand, which is able to coordinate in both mono- and bridging fashions to metal centers. The dimeric rhodium complex can be converted into the monomeric complex, but conversion of the iridium complex was unsuccessful in our hands. As shown by the X-ray crystal structure for the monomeric rhodium complex, dpdpc produces a very acute bite angle between P–Rh–P of 71.6°. These results are worthy of further investigations which are ongoing in our laboratories.

5. Supplementary material

CCDC 716707 and 716708 contain the supplementary crystallographic data for compounds **2** and **1a**, respectively. These data can be obtained free of charge from The Cambridge Crystallographic Data Centre via www.ccdc.cam.ac.uk/data_request/cif.

Acknowledgements

We would like to acknowledge the Donors of the American Chemical Society Petroleum Research Fund and Fort Lewis College for support of this research.

References

[1] J.-H. Xie, Q.-L. Zhou, Acc. Chem. Res. 41 (2008) 581–593.
[2] T. Jerphagnon, J.-L. Renaud, C. Bruneau, Tetrahedron Asymmetry 15 (2004) 2101–2111.
[3] P. Laurent, N. Le Bris, H. Des Abbayes, Trends Organomet. Chem. 4 (2002) 131–139.
[4] R.B. King, J. Organomet. Chem. 557 (1998) 29–35.
[5] P.E. Garrou, Chem. Rev. 85 (1985) 171–185.
[6] I. Tkatchenko, Phosphorus, Sulfur Silicon Relat. Elem. 18 (1983) 311–314.
[7] J. Ledford, C.S. Shultz, D.P. Gates, P.S. White, J.M. DeSimone, M. Brookhart, Organometallics 20 (2001) 5266–5276.
[8] P.W.N.M. van Leeuwen, P.C.J. Kamer, J.N.H. Reek, P. Dierkes, Chem. Rev. 100 (2000) 2741–2769.
[9] P.J. Brooks, M.J. Gallagher, A. Sarroff, M. Bowyer, Phosphorus, Sulfur Silicon Relat. Elem. 44 (1989) 235–247.
[10] M.E. Cucciolito, V. De Felice, I. Orabona, A. Panunzi, F. Ruffo, Inorg. Chim. Acta 343 (2003) 209–216.
[11] T.S. Morey, S.M. Miller, M.L. Helm, Acta Crystallogr., Sect. E: Struct. Rep. Online E63 (2007) m1983.
[12] L.J. Mason, E.M. Perrault, S.M. Miller, M.L. Helm, Inorg. Chem. Commun. 9 (2006) 946–948.
[13] V. De Felice, N. Fraldi, G. Roviello, F. Ruffo, A. Tuzi, J. Organomet. Chem. 692 (2007) 5211–5220.
[14] G.J. Grant, J.P. Lee, M.L. Helm, D.G. VanDerveer, W.T. Pennington, J.L. Harris, L.F. Mehne, D.W. Klinger, J. Organomet. Chem. 690 (2005) 629–639.
[15] W. Keim, P. Kraneburg, G. Dahmen, G. Deckers, U. Englert, K. Linn, T.P. Spaniol, G. Raabe, C. Krueger, Organometallics 13 (1994) 3085–3094.
[16] X-ray, Acta Crystallogr., Sect. A: Found. Crystallogr. 51 (1995) 33.
[17] G.M. Sheldrick, SHELXTL Version 6.12, Bruker Analytical X-ray Systems Inc., Madison, Wisconsin, USA, 2005.